



## Design and synthesis of pyridone inhibitors of non-nucleoside reverse transcriptase

Robert Gomez<sup>a,\*</sup>, Samson Jolly<sup>a</sup>, Theresa Williams<sup>a</sup>, Thomas Tucker<sup>a</sup>, Robert Tynebor<sup>a</sup>, Joe Vacca<sup>a</sup>, Georgia McGaughey<sup>b</sup>, Ming-Tain Lai<sup>c</sup>, Peter Felock<sup>d</sup>, Vandna Munshi<sup>c</sup>, Daniel DeStefano<sup>d</sup>, Sinoeun Touch<sup>c</sup>, Mike Miller<sup>d</sup>, Youwei Yan<sup>e</sup>, Rosa Sanchez<sup>f</sup>, Yuexia Liang<sup>f</sup>, Brenda Paton<sup>f</sup>, Bang-Lin Wan<sup>f</sup>, Neville Anthony<sup>g</sup>

<sup>a</sup> Department of West Point Discovery Chemistry, Merck Research Labs., 770 Sumneytown Pike, PO Box 4, West Point, PA 19486-0004, United States

<sup>b</sup> Department of Chemistry Modeling and Informatics, Merck Research Labs., 770 Sumneytown Pike, PO Box 4, West Point, PA 19486-0004, United States

<sup>c</sup> Department of In Vitro Pharmacology, Merck Research Labs., 770 Sumneytown Pike, PO Box 4, West Point, PA 19486-0004, United States

<sup>d</sup> Department of ID Antiviral HIV Discovery, Merck Research Labs., 770 Sumneytown Pike, PO Box 4, West Point, PA 19486-0004, United States

<sup>e</sup> Department of Structural Chemistry, Merck Research Labs., 770 Sumneytown Pike, PO Box 4, West Point, PA 19486-0004, United States

<sup>f</sup> Department of DMPK Preclinical WP, Merck Research Labs., 770 Sumneytown Pike, PO Box 4, West Point, PA 19486-0004, United States

<sup>g</sup> Department of Boston Discovery Chemistry, Merck Research Labs., 33 Avenue Louis Pasteur, Boston, MA 02115-5727, United States

### ARTICLE INFO

#### Article history:

Received 9 August 2011

Revised 5 October 2011

Accepted 7 October 2011

Available online 17 October 2011

#### Keywords:

Non-nucleoside reverse transcriptase

inhibitor

Pyridone

Pyridinone

HIV

### ABSTRACT

Next generation NNRTIs are sought which possess both broad spectrum antiviral activity against key mutant strains and a high genetic barrier to the selection of new mutant viral strains. Pyridones were evaluated as an acyclic conformational constraint to replace the aryl ether core of MK-4965 (**1**) and the more rigid indazole constraint of MK-6186 (**2**). The resulting pyridone compounds are potent inhibitors of HIV RT and have antiviral activity in cell culture that is superior to other next generation NNRTI's.

© 2011 Elsevier Ltd. All rights reserved.

HIV (human immunodeficiency virus) has a high rate of mutation due to its infidelity during replication. As a result, single drug therapy is ineffective due to the rapid selection of resistant mutant viral strains.<sup>1</sup> The more effective regimen, highly active antiretroviral therapy (HAART), uses at least two anti-HIV drugs simultaneously. This therapy significantly reduces HIV viral load and has led to a dramatic decrease in AIDS related mortality.<sup>2</sup> The emergence of HIV-1 strains resistant to at least one antiretroviral drug highlights the need for further development of antiviral agents with improved efficacy against these mutant strains.<sup>3</sup>

Reverse transcriptase (RT) inhibitors block the conversion of single stranded viral RNA to double stranded DNA, a prerequisite to integration into host DNA.<sup>4</sup> Non-nucleoside reverse transcriptase inhibitors (NNRTIs) interact with the RT enzyme at an allosteric site to induce a change in the substrate binding site which interferes with polymerase activity.<sup>5</sup> A common consequence of NNRTI use is the emergence of resistant mutant forms of HIV.<sup>6</sup>

\* Corresponding author. Tel.: +1 215 652 4715; fax: +1 215 652 3971.

E-mail address: [Robert\\_gomez@merck.com](mailto:Robert_gomez@merck.com) (R. Gomez).

Next generation NNRTIs are sought which possess both broad spectrum antiviral activity against key mutant strains (especially K103N and Y181C) and a high barrier to the selection of new mutant strains. Additionally, facilitating patient compliance dictates that next generation NNRTIs are efficacious with once daily oral administration. The current leader in the pursuit of improved NNRTI's is Tibotec's Rilpivirine<sup>®</sup> (TMC278)<sup>7</sup> which was recently approved by the FDA to be administered orally once daily.

In recent years, several groups have reported NNRTI's which feature a biaryl ether.<sup>8</sup> Specifically, Tucker et. al. reported a series of biaryl ethers (Fig. 1) which feature a pyrazolopyridine, as exemplified by MK-4965 (**1**), and have excellent broad spectrum antiviral activity against key mutant strains of RT. We<sup>9</sup> have also shown that conformationally constrained inhibitors (Fig. 1) such as MK-6186 (**2**) have comparable antiviral activity with good pharmacokinetics when dosed orally to preclinical species. Visual inspection of the X-ray crystal structures of **1** (PDB entry 3DRP) and **3**, a benzotriazole analog of **2** containing an aminomethyl group, complexed to wt RT (Fig. 2) shows the importance of the positioning of the pyrazolopyridine moiety with respect to the central phenyl ring

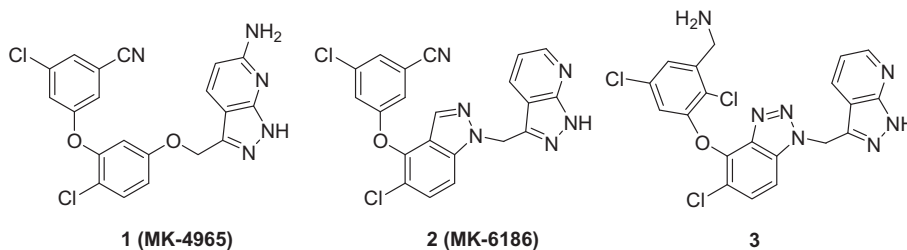


Figure 1. Structures of lead NNRTI inhibitors.

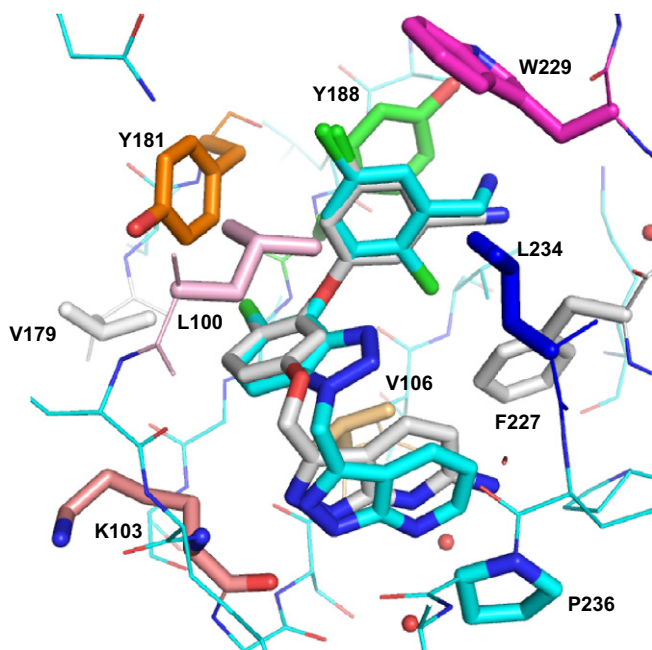


Figure 2. The bound conformation of **3** (teal) (from crystal structure complex with wt-RT) superimposed with the crystal structure of **1** (gray) complexed with wt-RT (PDB entry 3DRP). Active site residues within 7 Å are displayed. Key active site residues are highlighted and labeled in black. W239 and Y318 are hidden for clarity.

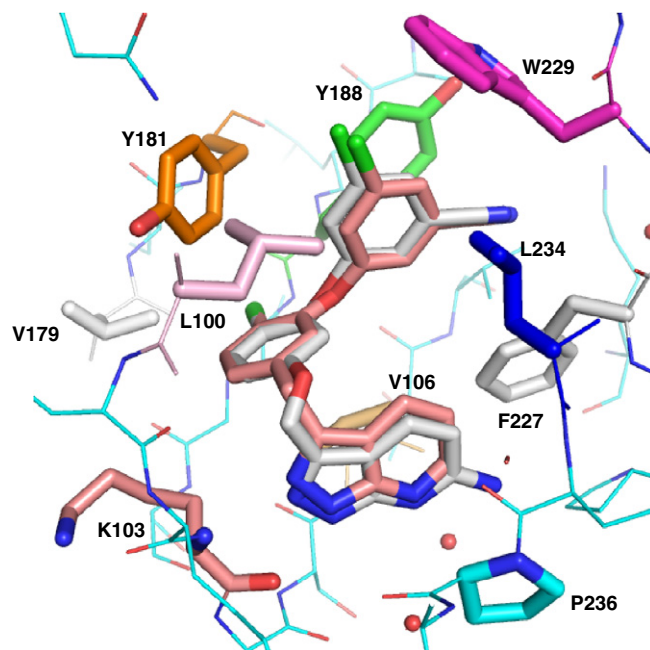


Figure 4. Docked conformation of **5** (salmon) superimposed with the bound conformation of **1** (gray) complexed with wt RT. Active site residues within 7 Å are displayed. Key active site residues are highlighted and labeled in black. W239 and Y318 are hidden for clarity.

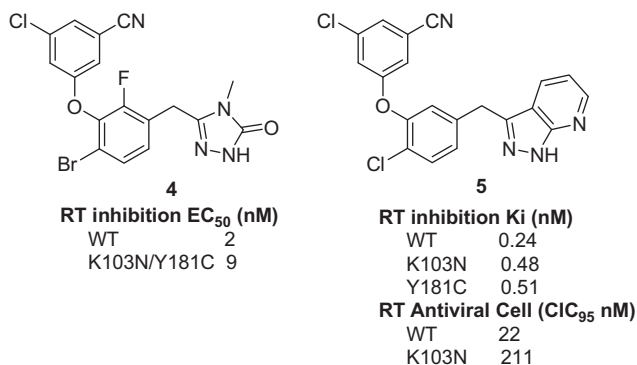


Figure 3. Structures and RT inhibition of methylene linked NNRTI inhibitors.

as the resulting hydrogen bonds to the K103 backbone are essential for binding. The bound conformations of **1** and **3** complexed with wt RT show dihedral angles of 150° and 180° with respect to the linker between the pyrazolopyridine and the central phenyl ring.

Sweeney et. al.<sup>10</sup> have found that methylene linked inhibitors such as **4** (Fig. 3) are potent inhibitors of RT. These compounds contain a triazolone moiety which presumably forms hydrogen bond

interactions with the K103 backbone in an analogous fashion to the pyrazolopyridine of **1** and **3**. We<sup>11</sup> and others<sup>12</sup> have shown that one atom linkers between the pyrazolopyridine and the central phenyl ring are also potent inhibitors of RT. In particular, the methylene linked **5** (Fig. 3) has sub-nanomolar enzyme inhibition against both wt-RT and the two most clinically relevant mutants, K103N and Y181C. Compound **5** was docked<sup>13</sup> in the binding site of **1** complexed with wt-RT. This docked conformation of **5** is superimposed with the bioactive conformation of **1** (Fig. 4) and shows exceptional alignment of the terminal rings. The linker to the pyrazolopyridine of the docked conformation of **5** shows a dihedral angle of 81° with respect to the central ring and indicates the need for a nearly orthogonal disposition for a one atom linker relative to the central core ring. This contrasts with the bound conformations of the 2 atom linked inhibitors, **1** and **3**, which are more planar with the linkers having measured dihedral angles of 150° and 180° with respect to the central ring. **5** was unfortunately less active in cell culture than **1**, especially against the virus containing the K103N mutant (211 nM), and had suboptimal pharmacokinetics in rat. These shortcomings may be due to the nature of the central phenyl ring and linker since the related compounds **1** and **2** have superior profiles. We sought to change the nature of the central ring and linker of **5** in order to improve the antiviral activity in cell culture and the pharmacokinetics in our preclinical species.

Pyridones are a common platform used in drug development<sup>14</sup> because their increased polarity is often more favorable than their phenyl counterparts and the amide linkage leads to the possibility of generating hydrogen bond interactions to increase affinity. Computational analysis of *N*-alkyl pyridones<sup>15</sup> shows a distinct conformational preference in accordance with other *ortho* substituted aromatics. A dihedral torsion driver was performed on *N*-ethyl pyridone (blue curves) as shown in Figure 5. Minimization of the steric interactions of the pyridone carbonyl with the ethyl group leads to an energy minimum at a dihedral angle of 90°. This contrasts the synperiplanar disposition (dihedral angle of 0°) which is predicted to be 6 kcal/mol higher in energy. The orthogonal arrangement compliments the predicted bioactive conformation of **5** from the docking study.<sup>12</sup>

A dihedral torsion driver was likewise performed on methoxybenzene<sup>15</sup> to better understand the conformational preferences of the oxymethylene linker of **1** as shown in Figure 5. Contrasting the pyridone, the energy minima of methoxybenzene are at dihedral angles of 0° and 180°. As anticipated, these planar dispositions are the result of non-bonding lone pair electron conjugation with the benzene ring. The observed dihedral angle of 150° for oxymethylene ether **1** complexed with wt RT is predicted to be only 0.5 kcal/mol from the energy minima at the dihedral angle 180°.

The central rings of **1** and **5** were replaced by a pyridone ring as in Figure 6. We anticipated that the carbonyl oxygen atom of the pyridone would be well tolerated as the benzotriazole nitrogen atoms of **3** are accommodated in the binding site. The methylene analog ( $n = 1$ ) would be predicted from the dihedral torsion driver of *N*-ethyl pyridone and docking studies of **5** to be a good match for the bioactive conformation. The orthogonal placement is the low energy conformation that is necessary for proper alignment of the pyrazolopyridine with K103 backbone. The ethylene analog ( $n = 2$ ), however, was expected to be less compatible with the bioactive conformation as the 150° dihedral angle optimal for proper alignment of the pyrazolopyridine for two atom linkers would be energetically unfavorable. The torsional strain for accessing the bioactive conformation in this case is predicted to be 3.0 kcal/mol.

The chemistry was first examined in the context of the 4-methyl pyridone analogs to afford **6** and **7**. This synthetic approach was then adapted to prepare the corresponding 4-chloro analog **8** as outlined in Scheme 1.<sup>16</sup> The reactivity of 4-chloropyridines toward  $S_NAr$  reactions necessitated the introduction of an activating

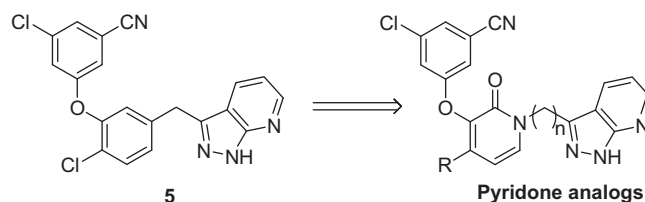


Figure 6. Pyridone class of NNRTI inhibitors from **5**.

group at the *ortho* position to direct the pyridine precursors toward displacements at the required *meta* position. As such, 3-fluoro-4-chloro pyridine (**11**) was deprotonated with lithium tetramethylpiperide<sup>17</sup> in hexanes and then quenched with bromine to give the 2-bromopyridine **12**. This bromide was cyanated with zinc cyanide and catalytic palladium(0) to provide the suitably activated 2-cyanopyridine **13**. Heating **13** and 3-bromo-5-chlorophenol to 55 °C with  $K_2CO_3$  as base gave only the desired displacement product **14**. The nitrile was then hydrolyzed to acid **15** using concentrated HCl at 100 °C. Curtius rearrangement of the azide derived from carboxylic acid **15** using diphenyl phosphorylazide (dppa) with *t*-butanol provided the Boc protected aminopyridine **16**. This aryloxy bromide was then cyanated using zinc cyanide in the presence of a palladium(0) catalyst and the Boc group deprotected with TFA to give the aminopyridine **17**. The aminopyridine was converted to the hydroxypyridine **18** via the hydrolysis of the corresponding diazonium salt in sulfuric acid. This hydroxypyridine was selectively *N*-alkylated with bromide **19** to provide, after deprotection, **8**. The corresponding 4-methyl analog **6** was made in a similar manner starting with the commercially available 2-bromo-3-fluoro-4-methylpyridine.

The synthetic approach used to prepare the ethylene linked analog **7** is outlined in Scheme 2. The bromide **19** was treated with NaCN in DMF to provide a mixture of products including the Boc and des Boc desired product as well as by products derived from alkylation of prematurely deprotected pyrazolopyridine. This mixture was deprotected with TFA and the resulting mixture was purified to provide **20**. This nitrile was hydrolyzed with concd HCl at 100 °C and the resulting carboxylic acid esterified in MeOH to provide the ester **21**. The pyrazolopyridine was protected with THP by treatment with DHP and DDQ to provide **22**. The methyl ester was reduced with LAH in THF to provide the requisite

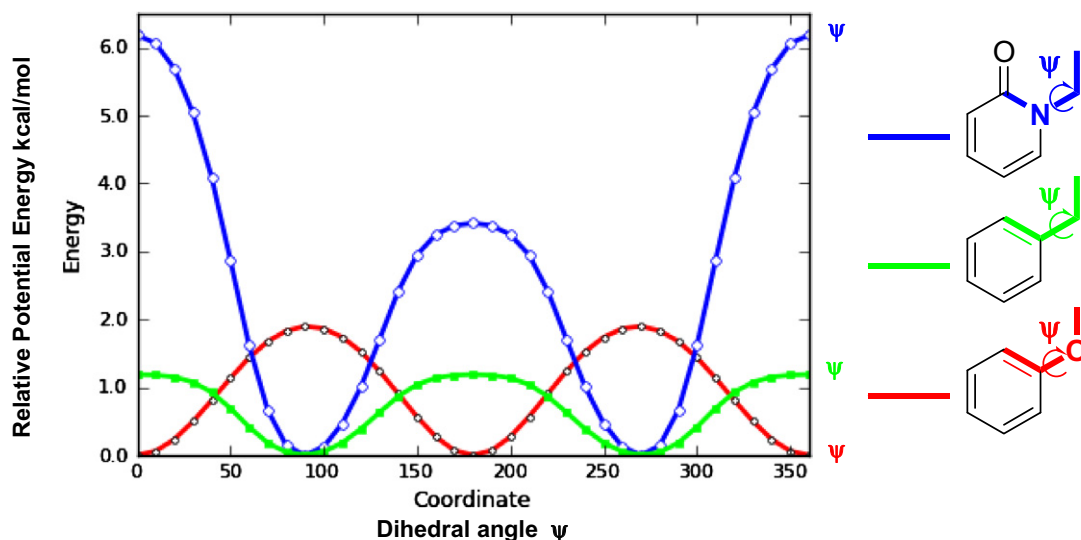
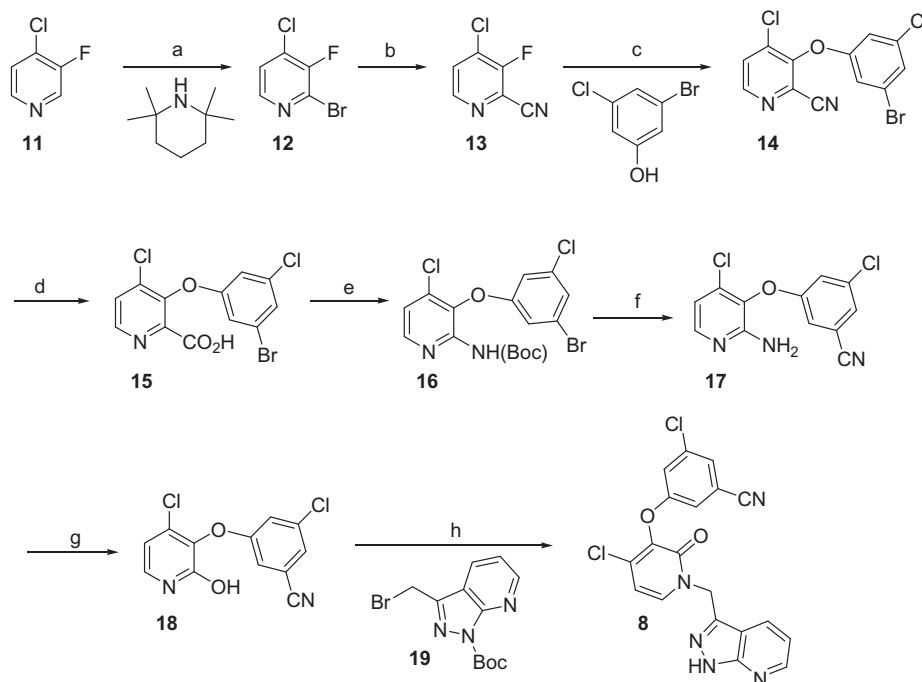
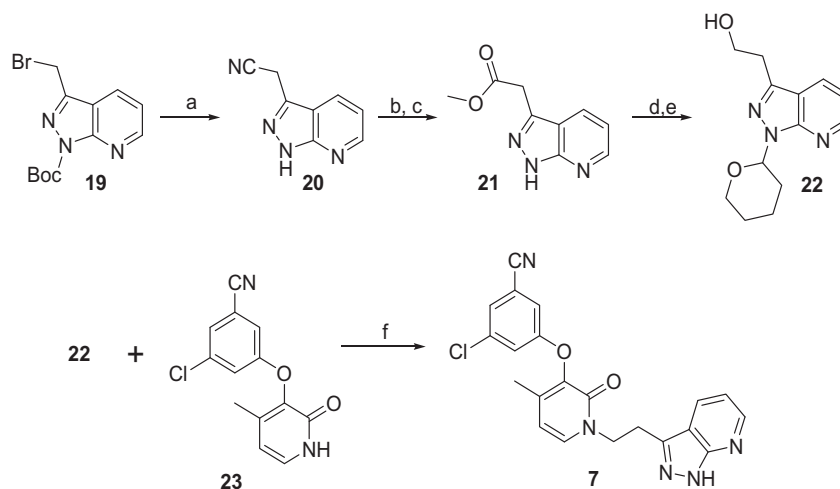


Figure 5. Dihedral torsional energy drivers for *N*-ethylpyridone, ethylbenzene and methoxybenzene.



**Scheme 1.** Synthesis of 4-chloropyridone **8**. Reagents and conditions: (a) BuLi, hexanes,  $-78^{\circ}\text{C}$ , then  $\text{Br}_2$ , 39%; (b)  $\text{Zn}(\text{CN})_2$ , cat  $\text{Pd}(\text{PPh}_3)_4$ , DMF,  $100^{\circ}\text{C}$ , 2 h, 40%; (c)  $\text{K}_2\text{CO}_3$ , DMF,  $55^{\circ}\text{C}$ , 20 min, 100%; (d) concd HCl,  $100^{\circ}\text{C}$ , 2 h, 83%; (e)  $\text{dppa}$ ,  $t\text{-BuOH}$ , pyridine, TEA,  $65^{\circ}\text{C}$ , 1 h, 59%; (f)  $\text{Zn}(\text{CN})_2$ , cat  $\text{Pd}(\text{PPh}_3)_4$ , NMP,  $90^{\circ}\text{C}$ , 1 h, then TFA, 71%; (g)  $\text{NaNO}_2$ ,  $\text{H}_2\text{SO}_4$ , 87%; (h)  $\text{K}_2\text{CO}_3$ , DMF,  $55^{\circ}\text{C}$ , 2 h, TFA, 92%.



**Scheme 2.** Synthesis of ethylene linked **7**. Reagents and conditions: (a) NaCN, DMF, rt, 2 h, then TFA, 20%; (b) concd HCl,  $100^{\circ}\text{C}$ , 30 min, 66%; (c)  $\text{HCl}(\text{g})$ , MeOH, 86%; (d) DHP, DDQ, ACN,  $85^{\circ}\text{C}$ , 1 h, 90%; (e) LAH, THF,  $0^{\circ}\text{C}$ , 76%; (f) DIAD,  $\text{PPh}_3$ , THF then TFA, 18%.

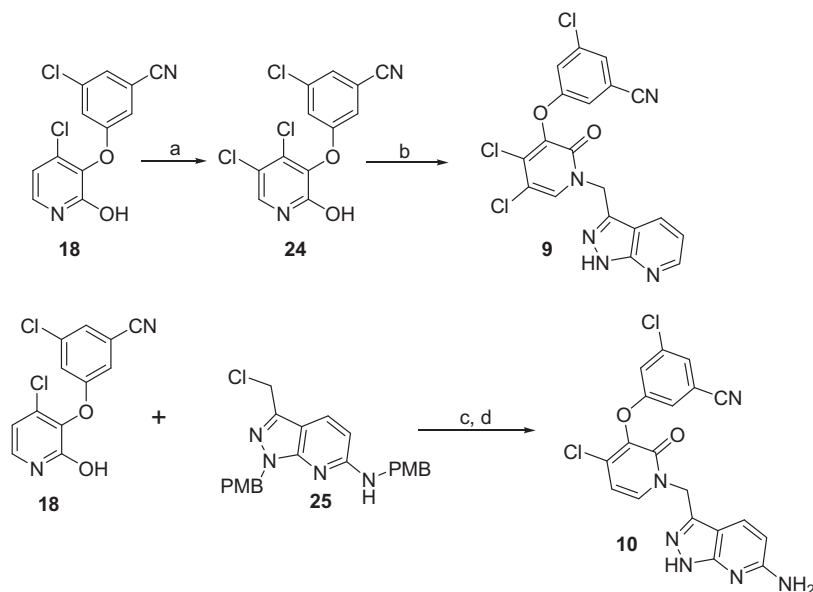
hydroxyethyl pyrazolopyridine **23**. Mitsunobu reaction of **23** with the methylpyridone **24** followed by TFA deprotection provided **7**.

The key synthetic steps to prepare **9** and **10** are outlined in Scheme 3. The 4-chloro pyridone **18** was selectively chlorinated using NCS in AcOH at  $60^{\circ}\text{C}$  to give the bischloro pyridone **24**. This pyridone was alkylated with bromide **19** in DMF at  $55^{\circ}\text{C}$  and then deprotected with TFA to afford **9**. The 6-aminopyrazolopyridine **10** was prepared from **18** via alkylation with chloride **25** and subsequent TFA deprotection at  $75^{\circ}\text{C}$ .

Table 1 details the data for the pyridone analogs relative to the oxymethylene linked **1**. Compounds were evaluated for intrinsic enzyme inhibitory potency<sup>18</sup> versus wt RT as well as the K103N and Y181C mutant variants. Compounds were also evaluated for antiviral potency<sup>19</sup> ( $\text{IC}_{95}$ ) against wt and the key mutant viruses

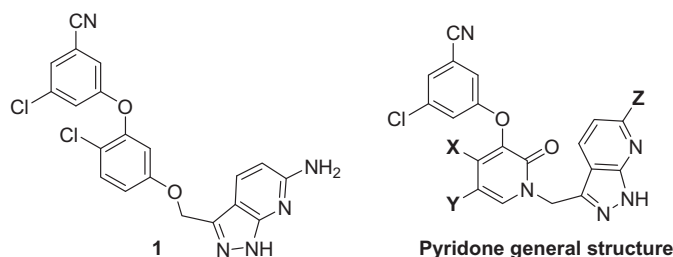
in the presence of 10% fetal bovine serum (FBS) as well as with 50% normal human serum (NHS) to evaluate the effects of protein binding.

The 4-methyl pyridone **6** was initially prepared due to its synthetic tractability relative to the corresponding 4-chloro analog. The 4-methyl pyridone **6** was 10-fold less potent in the enzyme inhibition assay than MK-4965 (**1**) against wt RT and the clinically relevant mutants, K103N and Y181C. Despite this loss in intrinsic potency against RT, **6** had greater antiviral activity in cell culture than **1** against wt, the K103N and Y181C mutant viruses as well as the double mutant, K103N/Y181C. The improved ratio between enzyme inhibition and antiviral activity in cell culture suggests that the pyridone is less encumbered by non-specific binding. In addition, the potency of **6** is shifted only 3.3-fold in the antiviral



**Scheme 3.** Synthesis of compounds **9** and **10**. Reagents and conditions: (a) NCS, AcOH, 60 °C, 2 h, 87%; (b) **19**, K<sub>2</sub>CO<sub>3</sub>, DMF, 55 °C, 30 min, then TFA, 86%; (c) K<sub>2</sub>CO<sub>3</sub>, DMF, 55 °C, 2 h, then TFA, 75 °C, 2 h, 85% (2 steps).

**Table 1**  
Enzyme inhibition and antiviral activity of pyridones **6–10** and compound **1**



Compd	X	Y	Z	n	Inhibition of RT polymerase, K <sub>i</sub> <sup>a</sup> (nM)			Antiviral activity in cell culture, IC <sub>95</sub> <sup>b</sup> (nM)				
					WT	K103N	Y181C	WT	K103N	Y181C	K103N/Y181C	WT, 50%NHS
<b>1</b>	—	—	—	—	0.20	0.39	0.39	5.0	12	27	73	28
<b>6</b>	Me	H	H	1	2.5	3.7	3.1	3.6	10	n.d.	31	12
<b>7</b>	Me	H	H	2	25	58	51	248	447	n.d.	n.d.	611
<b>8</b>	Cl	H	H	1	<b>0.77</b>	<b>1.5</b>	<b>1.0</b>	<b>2.4</b>	<b>2.9</b>	<b>7.8</b>	<b>7.0</b>	<b>7.7</b>
<b>9</b>	Cl	Cl	H	1	1.0	1.6	1.3	4.6	11	15	31	15
<b>10</b>	Cl	H	NH <sub>2</sub>	1	1.3	2.1	1.8	1.9	7.1	63	30	11

<sup>a</sup> Compounds were evaluated in a standard SPA assay. Values are the geometric mean of at least two determinations. Assay protocols are detailed in Ref. 18.

<sup>b</sup> IC<sub>95</sub>(cell culture inhibitory concentration) is defined as the concentration at which the Spread of virus is inhibited by >95% in MT-4 human T-lymphoid cells maintained at RPMI 1640 medium containing either 10% FBS or 50% NHS. Details of the assay are provided in Ref. 19. Values are the geometric mean of at least 2 determinations. n.d. = not determined. No cytotoxicity was observed for any of the compounds up to the upper limit of the assay (8.3 μM).

assay in the presence of normal human serum which is consistent with its moderate plasma protein binding.

The crystal structure of **6**<sup>20</sup> complexed with the K103N RT (PDB code 3TAM) has been determined at a resolution of 2.5 angstroms (Fig. 7). The terminal benzonitrile ring fills a large lipophilic pocket in the allosteric site formed by Y181, Y188, W229, L234 and F227. The two faces of the pyridone ring interact with V106 and L100, respectively, while the methyl containing edge interacts with V179 and Y181. Importantly, the key backbone interactions between K103 and the pyrazole nitrogens, which are critical for binding, are maintained. Interestingly, the aryl rings of the bioactive conformation of pyridone **6** are shifted 0.5–1.0 angstroms relative to the corresponding rings in the crystal structure of biaryl ether **1**.

The ethylene linked pyridone analog **7** was 10-fold less potent than **6** in the enzyme inhibition assay and had 50-fold less antiviral

activity in cell culture. This loss of binding and antiviral activity correlates with the increased torsional strain needed for the ethylene linked pyridone to adopt the bioactive conformation.

The chloro substituent was one of the most potent substituents in the oxymethylene series<sup>21</sup> and was incorporated into the pyridone series. The resulting 4-chloro pyridone **8** was 3-fold more potent an inhibitor of RT than **6** against both wt and the clinically relevant mutants, K103N and Y181C. As a consequence, **8** had significantly greater antiviral activity in cell culture than **6**. Importantly, **8** had 10-fold more antiviral activity than **1** against the K103N/Y181C double mutant virus.

The bis chloro pyridone **9** had slightly reduced intrinsic enzyme inhibition against wt and the K103N and Y181C mutant viruses. The additional chloro group particularly affects cell activity leading to a 2-fold reduction in potency against the wt and mutant viruses.

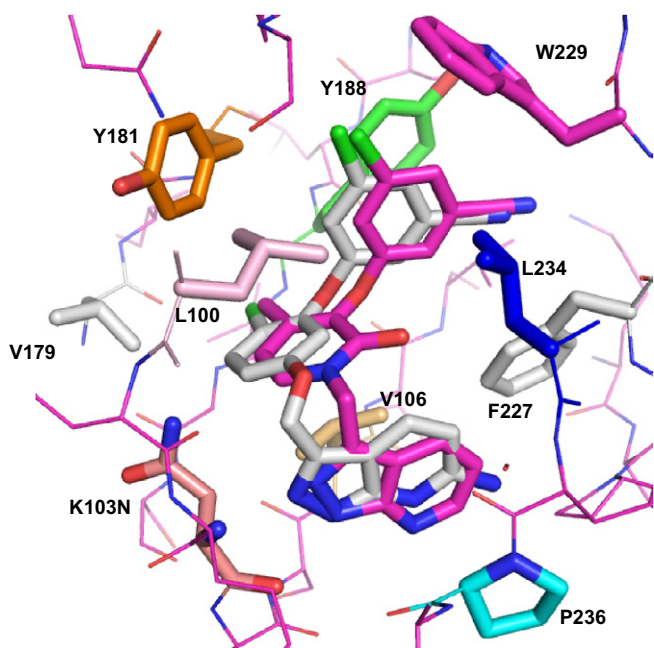


**Figure 7.** The crystal structure of **6** (magenta) complexed with K103N mutant RT (PDB entry 3TAM) superimposed with the bound conformation of **1** (gray) (from PDB entry 3DRP). Key active site residues are highlighted and labeled in black. Active site residues P99 and Y318 are hidden for clarity.

Analogously to work leading to **1**,<sup>8</sup> the 6-amino group was incorporated onto the pyrazolopyridine of **8** to give compound **10**. This compound was also slightly less potent in intrinsic enzyme inhibition relative to **8** and also had significantly less antiviral activity against the Y181C and K103N/Y181C mutant viruses.

The pyridone **8** was evaluated for its antiviral potency versus a more extensive panel of clinically relevant mutant cell lines<sup>22,23</sup> and compared with **1** (MK-4965), Tibotec's TMC-278 and Pfizer's UK-453061. These activity profiles are illustrated in Figure 8 which shows the various mutants versus their respective IC<sub>50</sub> values for each of the compounds in the study. The IC<sub>50</sub> is defined as the concentration of compound in cell culture required to block 50% of viral replication. Pyridone **8** in purple had a distinctly better profile than both **1** (magenta) and UK-453061 (yellow). TMC-278 had a comparable profile to **8** except for the K101P/K103N double

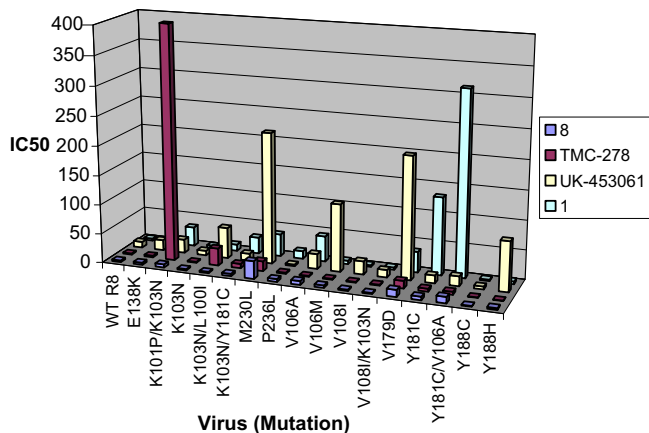


**Figure 8.** Antiviral potency of lead inhibitors versus panel of mutant cell lines. Compounds were analyzed in a Monogram Bioscience Phenoscreen assay using 10% FBS. The IC<sub>50</sub> is defined as the concentration of compound in cell culture required to block 50% of viral replication. Details provided in Ref. 23. WT R8 refers to a wild type cell line.

mutant in which TMC-278 had an IC<sub>50</sub> of >1 μM. This study demonstrates that **8** possesses a broad spectrum of activity against a variety of mutant viruses and appears to be an improved inhibitor compared to some of the best next generation NNRTIs.

Pyridone **8** was also evaluated for its antiviral potency of wt, the K103N and Y181C mutants and the K103N/Y181C double mutant viruses in 50% NHS and compared with **1**, TMC-278 and UK-453061. The use of 50% NHS is more relevant to the clinical environment and reflects the expected influence of plasma protein binding on the antiviral potency of these inhibitors. These antiviral activities in cell culture using 50% NHS are illustrated in Figure 9. For comparison, the potencies in 10% FBS are provided in parentheses. The shift in cell activity by changing from 10% FBS to 50% NHS was considerably greater for TMC-278 (20–30-fold) relative to **1** (5–6-fold), UK-453061 (2-fold) and **8** (3–4-fold except double mutant) reflecting their relative affinities for plasma protein.<sup>24</sup> Notably, the potency of **8** was superior to this collection of lead inhibitors and had about 4-fold greater antiviral activity than the other compounds when assayed in the presence of 50% NHS.

The pharmacokinetic parameters of the pyridone analogs was determined in rats and are tabulated in Table 2. Sprague Dawley rats received an intravenous (iv) dose as a solution in DMSO via an indwelling canula implanted in the jugular vein. Animals received an oral (p.o.) dose as a suspension in aqueous methylcellulose. The plasma concentrations of the compounds were determined by liquid chromatography mass spectral analysis and the absolute oral bioavailability was determined by comparing the mean area under the plasma concentration–time curve.

The pyridone class of inhibitors was characterized by achieving only low exposure following p.o. administration. The lone exception was **8** which had exposures in rat comparable to **1**. However, the observed exposures showed high inter animal variation

Cmpd	Antiviral activity in cell culture with 50% NHS CIC <sub>95</sub> (nM) <sup>a</sup>			
	WT	K103N	Y181C	K103N/Y181C
<b>8</b>	7.7 (2.3)	12 (2.9)	20 (7.8)	69 (7.0)
TMC-278	36 (1.9)	46 (1.5)	104 (3.6)	311 (10)
UK-453061	40 (21)	70 (32)	68 (23)	100 (38)
<b>1</b>	26 (5)	54 (12)	175 (27)	589 (102)

**Figure 9.** Antiviral activity using 50% NHS in cell culture. <sup>a</sup>CIC<sub>95</sub>(Cell culture inhibitory concentration) is defined as the concentration at which the Spread of virus is inhibited by >95% in MT-4 human T = lymphoid cells maintained in RPMI 1640 medium containing 50% NMS. Details of the assay are provided in Reference #. Values are the geometric mean of at least 3 determinations. No cytotoxicity was observed for any of the compounds. Values in parenthesis are CIC<sub>95</sub> using 10% FBS.

**Table 2**  
Pharmacokinetics in rat of the pyridones **6–10** relative to **1** (MK-4965)

Compd	Vd (L/kg)	Clp (ml/min/kg)	t <sub>1/2</sub> (h)	F %	AUC <sub>N</sub> (po) (μM·h)
<b>1</b> <sup>b</sup>	2.0	9	3.5	52	2.3
<b>6</b>	3.7	11	11.7	8.5	0.31
<b>7</b> <sup>c</sup>	0.6	31	0.75	—	—
<b>8</b>	2.0	12	4	57	1.6 <sup>a</sup>
<b>9</b>	27	27	19	0	0
<b>10</b>	0.8	12	1.4	6	0.15

Average of at least 2 Sprague Dawley rats dosed at 10 mpk PO (methocel suspension) and 2 mpk IV (DMSO) unless otherwise noted. All values are within 25% of the mean.

<sup>b</sup> is not determined.

<sup>a</sup> Variability in exposures AUC = 24, 2.3, 1.5 and 38 μM h to give a geometric mean of 16 ± 15.5.

<sup>b</sup> Average of 4 Sprague Dawley rats dosed at 10 mpk PO (methocel suspension) and 3 mpk IV (DMSO).

<sup>c</sup> Average of Sprague Dawley rats dosed at 1mpk IV (DMSO). No PO dosing in rats.

(>10-fold). This variability limits the potential of this compound for development.

Next generation NNRTIs are being sought which possess both broad spectrum antiviral activity against key mutant strains and a high genetic barrier to the selection of new mutant strains. Pyridones were evaluated as an acyclic conformational constraint to replace the aryl ether core of MK-4965 (**1**) and the more rigid indazole constraint of MK-6186 (**2**). The resulting pyridone class of compounds were similarly potent inhibitors of HIV RT in vitro but have superior antiviral activity in cell culture. This improved antiviral activity was especially apparent when assayed in the presence of 50% NHS. Further work aimed at increasing the bio-availability of the pyridone inhibitors will be presented in due course.

## Acknowledgments

We thank Dr. Steve Young for his guidance and mentorship of this work. The authors also thank Sandor Varga and Mike Bogusky for NMR support and Joan Murphy for exact mass determinations in support of this project.

## References and notes

- Coffin, J. M. *Cell* **1986**, *46*, 1; Perrino, F. W.; Preston, B. D.; Sandell, L. L.; Loeb, L. A. *Proc. Natl. Acad. Sci. U.S.A.* **1989**, *86*, 8343; Menendez-Arias, L. *Prog. Nucleic Acid Res. Mol. Biol.* **2002**, *71*, 91.
- Gulick, R. M.; Mellors, J. W.; Havlir, D.; Eron, J. J.; Meibohm, A.; Condra, J. H.; Valentine, F. T.; McMahon, D.; Gonzalez, C.; Jonas, L.; Emini, E. A.; Chodakewitz, J. A.; Isaacs, R.; Richman, D. D. *Ann. Intern. Med.* **2000**, *133*, 35.
- Little, S. J.; Holte, S.; Routy, J.-P.; Daar, E. S.; Markowitz, M.; Collier, A. C.; Koup, R. A.; Mellors, J. W.; Connick, E.; Conway, B.; Kilby, M.; Wang, L.; Whitcomb, J. M.; Hellmann, N. S.; Richman, D. D. *N. Engl. J. Med.* **2002**, *347*, 385; Richman, D. D.; Morton, S. C.; Wrinn, T.; Hellmann, N.; Berry, S.; Shapiro, M. F.; Bozzette, S. A. *AIDS* **2004**, *18*, 1393.
- de Bethune, M.-P. *Antiviral Res.* **2010**, *85*, 75.
- Sluis-Cremer, N.; Temiz, N. A.; Bahar, I. *Curr. HIV Res.* **2004**, *2*, 323.
- Cheung, P. K.; Wynhoven, B.; Harrigan, P. R. *AIDS Rev.* **2004**, *6*, 107; Tambuyzer, L.; Azijn, H.; Rimsky, L. T.; Vingerhoets, J.; Lecocq, P.; Kraus, G.; Picchio, G.; De Bethune, M.-P. *Antiviral Ther.* **2009**, *14*, 103.
- Arasteh, K.; Riege, R. A.; Yeni, P.; Pozniak, A.; Boogaerts, G.; van Heeswijk, R.; de Bethune, M.-P.; Peeters, M.; Woodfall, B. *Antiviral Ther.* **2009**, *14*, 713.
- (a) Tucker, T. J.; Sisko, J. T.; Tynebor, R. M.; Williams, T. M.; Felock, P. J.; Flynn, J. A.; Lai, M.-T.; Liang, Y.; McGaughey, G.; Liu, M.; Miller, M.; Moyer, G.; Munshi, V.; Perlow-Poehnel, R.; Prasad, S.; Reid, J. C.; Sanchez, R.; Torrent, M.; Vacca, J. P.; Wan, B.-L.; Yan, Y. *J. Med. Chem.* **2008**, *51*, 6503; (b) Zhan, P.; Liu, X.; Li, Z. *Curr. Med. Chem.* **2009**, *16*, 2876.
- Gomez, R. P.; Jolly, S.; Williams, T.; Vacca, J.; Torrent, M.; McGaughey, G.; Lai, M. T.; Felock, P.; Munshi, V.; DiStefano, D.; Flynn, J.; Miller, M.; Yan, Y.; Reid, J.; Sanchez, R.; Liang, Y.; Paton, B.; Wan, B. L.; Anthony, N.; *J. Med. Chem.*, in press, doi:10.1021/jm2010173.
- Sweeney, Z. K.; Acharya, S.; Briggs, A.; Dunn, J. P.; Elworthy, T. R.; Fretland, J.; Giannetti, A. M.; Heilek, G.; Li, Y.; Kaiser, A. C.; Martin, M.; Saito, Y. D.; Smith, M.; Suh, J. M.; Swallow, S.; Wu, J.; Hang, J. Q.; Zhou, A. S.; Klumpp, K. *Bioorg. Med. Chem. Lett.* **2008**, *18*, 4348.
- Tucker, T. J.; Tynebor, R. M. Unpublished results.
- Sweeney, Z. K.; Harris, S. F.; Arora, N.; Javanbakht, H.; Li, Y.; Fretland, J.; Davidson, J. P.; Billedeau, J. R.; Gleason, S. K.; Hirschfeld, D.; Kennedy-Smith, J. J.; Mirzadegan, T.; Roetz, R.; Smith, M.; Sperry, S.; Suh, J. M.; Wu, J.; Tsing, S.; Villaseñor, A. G.; Paul, A.; Su Heilek, G.; Hang, J. Q.; Zhou, A. S.; Jernelius, J. A.; Zhang, F.-J.; Klumpp, K. *J. Med. Chem.* **2008**, *51*, 7449.
- The ligand **5** was docked within a 10 Å grid centroid of **1**. The protein/ligand complex was minimized using the low mode/mixed-torsional sampling algorithm as implemented in Schrodinger, LLC v2009.1 with a distance dependent dielectric constant of 2 with the MMFFs force field.
- Dragovitch, S.; Prins, T. J.; Zhou, R.; Johnson, T. O.; Hua, Y.; Luu, H. T.; Sakat, S. K.; Brown, E. L.; Maldonado, F. C.; Tuntland, T.; Lee, C. A.; Fuhrman, S. A.; Zalman, L. S.; Patrik, A. K.; Matthews, D. A.; Wu, E. Y.; Guo, M.; Borer, B. C.; Nayyar, N. K.; Moran, T.; Chen, L.; Rejto, P. A.; Rose, P. W.; Guzman, M. C.; Doval Santos, E. C.; Lee, S.; McGee, K.; Mohajeri, M.; Liese, A.; Tao, J.; Kosa, M. B.; Liu, B.; Batugo, M. R.; Gleason, J. R.; Wu, Z. P.; Liu, J.; Meador, J. W.; Ferre, R. A. *J. Med. Chem.* **2003**, *46*, 4572.
- The dihedral torsion driver was performed using low mode/torsional sampling every 10° as implemented in Schrodinger, LLC v2009.1 with a distance dependent dielectric constant of 1 with the OPLS.2005 force field. The dihedral angle is formed by the relationship between the β atom of the linker and the central ring.
- Full experimental details of the synthesis of compounds **6–10** are provided in Tucker, T. J.; Tynebor, R.; Sisko, J. T.; Anthony, N. J.; Gomez, R.; Jolly, S. M. U.S. Patent Appl. US 2007/3769P, 2007.
- Marzi, E.; Bobbio, C.; Cottet, F.; Schlosser, M. *Eur. J. Org. Chem.* **2005**, *10*, 2116.
- Saggat, S. A.; Sisko, J. T.; Tucker, T. J.; Tynebor, R. M.; Su, D.-S.; Anthony, N. J. U.S. Patent Appl. US 2007/021442 A1, 2007.
- Vacca, J. P.; Dorsey, B. D.; Schleif, W. A.; Levin, R. B.; McDaniel, S. L.; Darke, P. D.; Zugay, J.; Quintero, J. C.; Blahy, O. M.; Roth, E.; Sardana, V. V.; Schlabac, A. J.; Graham, P. I.; Condra, J. H.; Gotlib, L.; Holloway, M. K.; Lin, J.; Chen, I.-W.; Vastag, K.; Ostovic, D.; Anderson, P. S.; Emini, E. E.; Huff, J. R. *Proc. Natl. Acad. Sci. U.S.A.* **1994**, *91*, 4096.
- The X-ray diffraction data of the K103N mutant RT and inhibitor **6** complex crystal (Fig. 7) were obtained at 2.5 Å resolution and refined to an R-factor of 0.193 and an R-free of 0.249. The structure has been deposited in the Protein Data Bank with a PDB code of 3TAM.
- Tucker, T. J.; Saggat, S.; Sisko, J. T.; Tynebor, R. M.; Williams, T. M.; Felock, P. J.; Flynn, J. A.; Lai, M. T.; Liang, Y.; McGaughey, G.; Liu, M.; Miller, M.; Moyer, G.; Munshi, V.; Perlow-Poehnel, R.; Prasad, S.; Sanchez, R.; Torrent, M.; Vacca, J. P.; Wan, B. L.; Yan, Y. *Bioorg. Med. Chem. Lett.* **2008**, *18*, 2959.
- Domoaal, R. A.; Demeter, L. M. *Int. J. Biochem Cell Biol.* **2004**, *36*, 1735.
- The compounds were evaluated in a Monogram Bioscience Phenosense assay versus a panel of clinically derived RT mutants in the presence of 10% fetal bovine serum. The IC<sub>50</sub> is defined as the concentration of compound in cell culture required to block 50% of viral replication. Values are derived from the average of two determinations. Assays were performed by Monogram Biosciences, South San Francisco, CA. Details of the assay protocols are available at [http://www.monogramhiv.com/phenosense\\_introduction.aspx](http://www.monogramhiv.com/phenosense_introduction.aspx).
- Human plasma protein binding was determined for the following compounds: TMC-278 99.7% bound,<sup>25</sup> **1** 96.5% bound,<sup>26</sup> **8** 96.7% bound and UK-453061 51% bound.
- <http://chembl.blogspot.com/2011/05/new-drug-approvals-2011-pt-xv.html>.
- Lai, M.-T.; Munshi, V.; Touch, S.; Tynebor, R. M.; Tucker, T. J.; McKenna, P. M.; Williams, T. M.; DeStefano, D. J.; Hazuda, D. J.; Miller, M. D. *Antimicrob. Agents Chemother.* **2009**, 2424.